Spiral wave meandering induced by fluid convection in an excitable medium

V. Pérez-Villar,* A. P. Muñuzuri, M. N. Lorenzo, and V. Pérez-Muñuzuri
Group of Nonlinear Physics, Faculty of Physics, University of Santiago de Compostela, E-15782 Santiago de Compostela, Spain
(Received 10 January 2002; published 20 September 2002)

An isothermal reaction-diffusion system is considered in a two-dimensional fluid medium within a gravitational field. Inhomogeneities in the concentration field of the species give rise to a fluid flow due to buoyancy forces. A two-dimensional reaction-diffusion-convection model of an excitable medium is presented. The influence of hydrodynamics on spiral wave dynamics is systematically studied. A kinematic model is also introduced to better understand the mechanisms involved here.

DOI: 10.1103/PhysRevE.66.036309 PACS number(s): 47.20.Bp, 47.70.Fw, 82.30.−b

I. INTRODUCTION

Active media have been exhaustively studied during recent decades because of the important role they play in pattern formation. Examples can be found almost everywhere in nature, from galaxies to colonies of bacteria such as the social amoeba *Dictiostelium discoideum*, as well as the cardiac muscle and signal propagation through nerves, among others [1]. In particular, chemically active media have been used frequently as a test tube to check out the properties of these structures. Many of them arise as a consequence of the particular properties of the waves propagating through the medium [2]. These waves can be organized in spatiotemporal structures, called spiral waves, that last forever while unperturbed. Spiral waves can play both a constructive role (e.g., social amoeba) and a destructive role (e.g., tachycardia in the cardiac muscle) [3]. Because the systems where they appear are so important in nature and, in particular, for human life, their properties have been exhaustively studied experimentally [mainly in the chemical Belousov-Zhabotinsky (BZ) reaction], numerically, and theoretically. Also, the effect of deterministic or stochastic external fields on their dynamics has been analyzed lately [4,5].

All these studies share the common property of considering that the system can only experience reaction and diffusion among the different species in the system. In nature, however, the processes of reaction and diffusion in a fluid medium are carried out in the presence of a gravitational field. The gradients of concentration of the different species involved in the reaction and the temperature gradients due to the thermal effects of the chemical reaction create inhomogeneities in the medium that give rise to macroscopic movements of the fluid that modify the spatiotemporal pattern that develops in the system. The existence of gradients of density and temperature as local sources of fluid convection in the fluid has been recognized by several authors [6,7]. More recently, the effect of forced convection induced by an external velocity field on excitable spiral wave dynamics has been studied numerically [8]. The effect of a steady shear flow on excitable media was investigated recently by Biktashev *et al.* [9], and it was found that the flow affects the excitable dynamics by blocking or disrupting the excitation waves. Experimentally, oscillatory convective vortices were discovered as a result of the interaction between two spiral waves in the BZ reaction [10].

Recently, we studied the propagation of a front in a gel-liquid system; the propagation of a front in the gel phase originates a convection flow in the liquid phase that perturbs the propagation of the front in the gel phase [11]. This paper deals with the modeling of spiral wave dynamics in a two-dimensional fluid excitable medium in the presence of a gravitational field parallel to the plane where the chemical reaction takes place. The regions of the medium before and after the front of the spiral wave are affected by the concentration gradients of the different chemical species, as well as gradients of temperature, giving rise to a local fluid flow caused by inhomogeneities. In this paper, only the gravitational effect is taken into account, leaving for a later study the effects of temperature gradients. In the first section, a particular reaction model is considered to be coupled with the Navier-Stokes equations to model our problem accurately. In the following section, a particular example is studied, a spiral wave is allowed to be influenced by these processes, and its behavior is dramatically modified as a result. Also a simple kinematic model is presented to explain the observed mechanisms.

II. MODEL

One of the causes of convective phenomena is the existence of a gradient of temperature [12]. When the temperature is kept constant all over the medium, convective phenomena can appear due to gradients of density in the presence of a gravitational field. The aim of this paper is to study the behavior of spiral waves in an active medium at constant temperature under the effect of a gravitational field by taking into account the convective currents induced by the gradients of density. We will consider a two-dimensional medium (x,z), with z along the gravity direction.

A. Equations of motion

A reaction-diffusion system is usually described by a set of partial differential equations such as

$$\frac{\partial \mathbf{q}}{\partial t} = \mathbf{Q}(\mathbf{q},\mu) + \mathbf{D}\nabla^2\mathbf{q}, \tag{1}$$

*Corresponding author. Email address: fmvpv@usc.es
http://chaos.usc.es

where $\mathbf{q}$ is the concentration vector for the different species in the active medium, $\mathbf{Q}(\mathbf{q},\mu)$ describes the source terms, $\mathbf{D}$ is a diagonal matrix containing the diffusion coefficients for each species of the system, and μ is the set of parameters characterizing the system.

When this system is affected by a gravitational field, the resulting set of equations describing the reaction-diffusion-convective system is

$$\left(\frac{\partial}{\partial t}+\mathbf{V}\cdot\boldsymbol{\nabla}\right)\mathbf{q}=\mathbf{Q}(\mathbf{q},\mu)+\mathbf{D}\boldsymbol{\nabla}^2\mathbf{q}, \tag{2}$$

$$\left(\frac{\partial}{\partial t}+\mathbf{V}\cdot\boldsymbol{\nabla}\right)\mathbf{V}=-\mathbf{g}\frac{\rho}{\rho_0}-\frac{1}{\rho_0}\boldsymbol{\nabla}p+\nu\boldsymbol{\nabla}^2\mathbf{V}, \tag{3}$$

where $\mathbf{V}$ is the fluid velocity, p the hydrostatical pressure, $\mathbf{g}$ the acceleration of gravity, ν the kinematic viscosity, and ρ the density of the fluid, which is a function of the position and of the concentration of the different species $\mathbf{q}$. The reference values for the density, ρ_0, and for the concentrations, $\mathbf{q}_0$, are taken in the homogeneous state where all concentrations are those of the equilibrium state of the system $[\mathbf{Q}(\mathbf{q},\mu)=\mathbf{0},\mathbf{V}=\mathbf{0}]$.

Equation (3) is the Navier-Stokes equation under the Oberbeck-Boussineq approximation. In order to close the previous set of equations a relationship between ρ and $\mathbf{q}$ has to be established.

For all the different species involved in an isothermal chemical reaction a change in the density has to be associated with a variation of the volume if the partial molal volumes of the products are different from those of the reactants, as the mass remains constant. Thus, a change of the concentrations from the equilibrium state, $\mathbf{q}_0$, may induce a variation of the density, in a linear approach, given by [7]

$$\varrho=\varrho_0+\left(\frac{\partial\varrho}{\partial\mathbf{q}}\right)_{\mathbf{q}_0}\cdot(\mathbf{q}-\mathbf{q}_0). \tag{4}$$

Introducing the vorticity by $\mathbf{W}=\boldsymbol{\nabla}\wedge\mathbf{V}$, with the geometry considered for our problem and the acceleration of gravity oriented along the z axis, we can write $\mathbf{V}=(V_x,0,V_z)$, $\mathbf{g}=(0,0,-g)$, and $\mathbf{W}=(0,-\omega,0)$, so Eq. (3) becomes

$$\left(\frac{\partial}{\partial t}+\mathbf{V}\cdot\boldsymbol{\nabla}\right)\omega=-\frac{g}{\rho_0}\frac{\partial\rho}{\partial x}+\nu\boldsymbol{\nabla}^2\omega. \tag{5}$$

The velocity $\mathbf{V}$ and the vorticity ω are related via the stream function ψ, defined for a two-dimensional system as

$$V_x=\frac{\partial\psi}{\partial z},\qquad V_z=-\frac{\partial\psi}{\partial x}, \tag{6}$$

which are related to the vorticity by $\omega=-\boldsymbol{\nabla}^2\psi$.

We considered that the reaction processes among the different species correspond to those of the Belousov-Zhabotinsky reaction [13,14]. Thus, we choose for the source terms $\mathbf{Q}(F,G,H)$ in Eq. (2) the three-variable Oregonator model given by

$$\begin{aligned}F(u,v,w)&=[w(u-q)+u-u^2]/\epsilon,\\ G(u,v,w)&=u-v,\\ H(u,v,w)&=[-w(q+u)+fv]/\epsilon',\end{aligned} \tag{7}$$

where (u,v,w) are the state variables representing the dimensionless concentrations of activator $[HBrO_2]$, catalyst [ferroin], and inhibitor $[Br^-]$, respectively, and f,q,ϵ,ϵ' are constants related to the chemical kinetics of the reaction [15]. For a typical recipe, we used a scaling with a spatial unit of 0.018 cm and a time unit of 21 s [6] using the "Lo" kinetic values given by Tyson [16]. Under this scaling, those constants are $f=1.4, q=0.002, \epsilon=0.01$, and $\epsilon'=0.001$. For this particular choice of parameters the Oregonator model exhibits oscillatory dynamics [17]. All hydrodynamic variables are expressed in terms of the scaling of Eq. (7). That is, $g=980\ \text{cm s}^{-2}\times(21\ \text{s})^2/(0.018\ \text{cm})=2.4\times10^7$, and $\nu=9.2\times10^{-3}\ \text{cm}^2\ \text{s}^{-1}\times(21\ \text{s})/(0.018\ \text{cm})^2=5.96\times10^2$. For our choice of parameters and in dimensionless form, the values for the state variables at equilibrium are $u_0=v_0=0.0116$ and $w_0=1.1942$.

In general, the density variation due to a change in the chemical composition is quite small for most known reactions. We may, therefore, assume a linear dependence of the density on the chemical concentrations and now write Eq. (4) as

$$\rho=\rho_0[1-\overline{V}_u(u-u_0)-\overline{V}_v(v-v_0)-\overline{V}_w(w-w_0)], \tag{8}$$

where $\overline{V}_u,\overline{V}_v$, and $\overline{V}_w$ are the partial molal volumes scaled using the "Lo" kinetic values, and represent the coefficients of linear expansion due to the compositional changes of $[HBrO_2]$, [ferroin], and $[Br^-]$, respectively. The three-variable Oregonator model is a very simplified model for the BZ reaction and it may not precisely account for all the chemical species that have an influence on the convective dynamics of the fluid; furthermore, there are no precise experimental results about the relative importance of $\overline{V}_u,\overline{V}_v$ and $\overline{V}_w$. In this paper we assume that the three values of $\overline{V}$ are the same as in [11], and set them equal to $\sigma=\overline{V}_u=\overline{V}_v=\overline{V}_w$, where σ is a *fictitious* molal volume that controls the wave front density. Then, Eq. (8) simplifies to

$$\rho=\rho_0[1-\sigma(u-u_0)-\sigma(v-v_0)-\sigma(w-w_0)]. \tag{9}$$

Positive values of σ are due to the fact that density values are smaller at the wave fronts where the reaction takes place than in the rest of the liquid solution [18]. The value of σ can be obtained from experimental measurements and it changes dramatically with the reaction or catalysts used. Typical values of σ for the BZ reaction are within the range $[10^{-6},10^{-2}]$ [7,16,19].

Finally, the set of equations describing the dynamics of the BZ reaction with convection is

$$\frac{\partial u}{\partial t}=F(\mathbf{x})+J(\psi,u)+D_u\boldsymbol{\nabla}^2u, \tag{10}$$

$$\frac{\partial v}{\partial t} = G(\mathbf{x}) + J(\psi, v) + D_v \nabla^2 v, \tag{11}$$

$$\frac{\partial w}{\partial t} = H(\mathbf{x}) + J(\psi, w) + D_w \nabla^2 w, \tag{12}$$

$$\frac{\partial \omega}{\partial t} = J(\psi, \omega) + \sigma g \left(\frac{\partial u}{\partial x} + \frac{\partial v}{\partial x} + \frac{\partial w}{\partial x} \right) + \nu \nabla^2 \omega, \tag{13}$$

$$\omega = -\nabla^2 \psi, \tag{14}$$

where the Jacobian operator is

$$J(f_1, f_2) = \frac{\partial f_1}{\partial x}\frac{\partial f_2}{\partial z} - \frac{\partial f_2}{\partial x}\frac{\partial f_1}{\partial z}. \tag{15}$$

The dimensionless diffusion coefficients D_u, D_v, and D_w of $[HBrO_2]$, [ferroin], and $[Br^-]$, respectively, were estimated from their molecular weights 113, 596, and 80 on the basis of the Stokes-Einstein relation. The diffusion coefficient is given by $D \sim M^{1/3}$ where M is the molecular weight. Then, taking into account the ratios $D_v/D_u = (113/596)^{1/3} = 0.6$ and $D_w/D_u = (113/80)^{1/3} = 1.1$, we set $D_u = 1$, $D_w = 1.1$, and $D_v = 0.6$ [20].

B. Initial and boundary conditions

Zero-flux boundary conditions for the chemical concentrations were used in all boundaries of the domain. For the stream function and vorticity the no-slip boundary condition was used.

The set of Eqs. (10)–(13) were integrated using an alternating direct implicit method, while Eq. (14) (a Poisson equation) was integrated using a full multigrid algorithm method [21]. The spatial step sizes were $\Delta x = \Delta z = 0.247$ step units (s.u). while the time step was $\Delta t = 10^{-4}$ time units (t.u.). The mesh sizes were in all cases $L_x \times L_z = 513 \times 513$.

Initially, chemical concentrations were assumed to be in steady state and convection free, except for an appropriate perturbation required to generate a spiral wave [22]. Thus, only Eqs. (10)–(12) were integrated with $\mathbf{V} = \mathbf{0}$ (i.e., no fluid flow). In this way, a steadily counterclockwise rotating spiral wave was created with its tip or free end following a circular trajectory with a period of rotation $T_0 = 3.28$ t.u. This state was used as an initial state for the chemical concentrations before convection was taken into account. Then, velocity, vorticity, and stream function were set equal to zero plus a random perturbation for all the mesh points.

III. RESULTS

Figure 1 shows the evolution of a spiral wave under the effect of a hydrodynamic field such as described in the previous section for $\sigma = 0.005$. Note that, for this particular value of σ, the density of the spiral waves and, in particular, that of the spiral tip is smaller than elsewhere in the fluid; thus, the spiral should move in the opposite direction to the gravitational field. Nevertheless, the spiral is observed to drift downward with a small velocity component in the perpendicular direction due to the chirality of the spiral. It is also possible to see that during its evolution the spiral structure is slightly distorted although the main geometry is preserved. The spiral wave tip shape is also not perturbed by the convective flow [Fig. 1(c)], as expected by the nearly linear drift and regular shape of the vortex. A change in the spiral chirality only introduces, as expected, a change in the per-

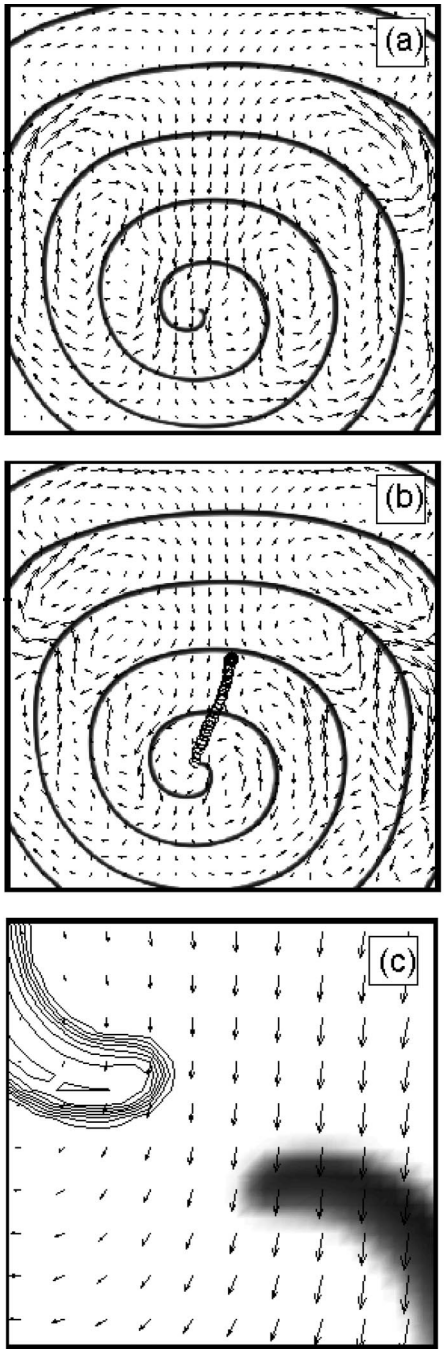

FIG. 1. Time evolution of a spiral wave and its corresponding hydrodynamic field for $\sigma = 0.005$. Superimposed in (b) the helical path followed by the spiral tip is represented. Note the formation of fluid vortices between the wave fronts. Panel (c) corresponds to an enlargement of the spiral wave tip (gray shaded) shown in (b). For comparison the same tip at 80 t.u. is also shown (contour line). Time periods: (a) 84.5 t.u. and (b) 85 t.u.

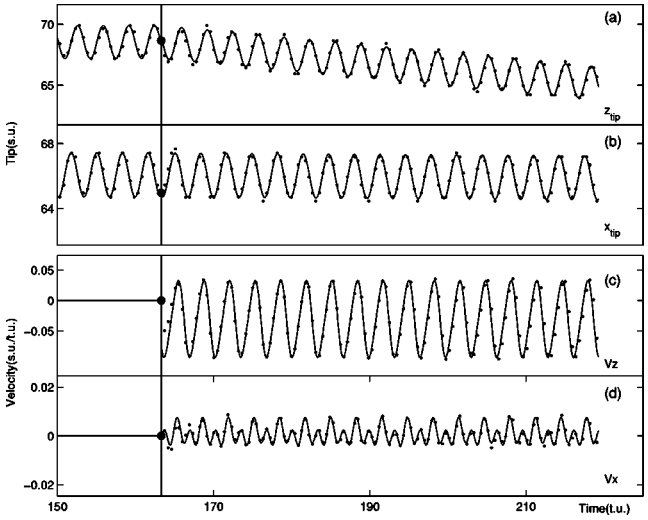

FIG. 2. Time evolution of the (x,z) position of the spiral tip (a),(b) and the velocity components (V_x, V_z) (c),(d) before and after the hydrodynamic field was set for $t=165$ t.u. and $\sigma=0.001$. Numerical data (dots) obtained after solving Eqs. (10)–(14) were fitted to a kinematic model, Eq. (16), shown by a solid line. Fitting parameters: $V_n^0=-4.23$, $V_t^0=-9.61$, $\delta_x=-3.75$, $\delta_z=1.99$, $a_0=3.8\times10^{-3}$, $a_1^c=-3.3\times10^{-3}$, $a_1^s=4.2\times10^{-3}$, $a_2^c=9.7\times10^{-5}$, $a_2^s=8.2\times10^{-3}$, $b_0=-0.12$, $b_1^c=-0.08$, $b_1^s=0.098$, $b_2^c=-0.013$, and $b_2^s=3.5\times10^{-3}$.

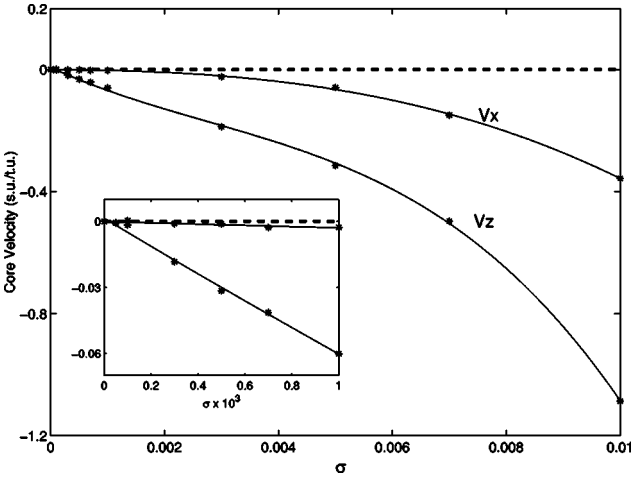

FIG. 3. Velocity of the core of the spiral wave as a function of the partial molal volume σ. The inset shows a magnification of the core velocity for small values of σ. Note that V_x is nearly zero for $\sigma<10^{-3}$.

pendicular direction of the motion (perpendicular to the direction determined by the gravitational field). Note as well that, due to the downward tip motion, the wavelength has diminished in the lower part of Fig. 1 when compared to the upper part as a consequence of a Doppler shift.

Because the density is smaller at the wave front than in the fluid between, convective vortices appear between fronts. The size of these vortices depends on the spiral wavelength and as the fronts evolve vortices reorganize as shown in the sequence of Figs. 1(a) and 1(b). In this sense, note for example that the streams at the left and right boundaries change direction in less that 0.5 t.u. since, as the fronts move, fluid density between the fronts and the boundaries decreases, so as to force the fluid to move downward due to buoyancy forces. So the rest of the vortices in the neighborhood reorganize to conserve vorticity. On the other hand, the vortices above do not change their positions but reorganize as the fronts pass. If the kinematical viscosity ν is diminished, only the flow velocities are increased, but the spiral wavelength and the front height, whose values depend on the chemical Oregonator model parameters, remain constant. In this case, the length scale of the flow rotating vortices is preserved and their vorticity increases.

The behavior of the tip far from the boundaries is shown in Fig. 2. Note that, after the hydrodynamic field is set, its effect induces a deviation of the trajectory of the tip, while the rotation period of the spiral wave remains constant. The components of the fluid velocity at the tip position (V_x, V_z) have an oscillatory behavior, with a negative mean value for V_z which is responsible for the opposite tip motion against the buoyancy forces.

Trying to identify the mechanisms involved here, we have developed a kinematic model [23] where the hydrodynamic effects (mainly described by the fluid velocity close to the tip) have been included. The tip trajectory followed by the spiral wave under hydrodynamical forcing can be described in terms of the equations of motion

$$\begin{pmatrix} \dot{x} \\ \dot{z} \end{pmatrix} = \begin{pmatrix} -\sin\nu_0 t & -\cos\nu_0 t \\ \cos\nu_0 t & -\sin\nu_0 t \end{pmatrix} \begin{pmatrix} V_n^0 \\ V_t^0 \end{pmatrix} + \begin{pmatrix} \delta_x V_x \\ \delta_z V_z \end{pmatrix}, \tag{16}$$

where the first term on the right-hand side in Eq. (16) describes the circular trajectory followed by the spiral wave tip before the convection effects were taken into account. The second term describes these effects and (V_x, V_z) are the fluid velocity components at the tip position (x,z). $\nu_0=2\pi/T_0$ and (δ_x, δ_z) are free parameters that account for the strength of the hydrodynamic contribution.

The normal and tangential velocities V_n^0 and V_t^0 were obtained by fitting the (x,z) positions of the spiral wave tip shown in Figs. 2(a) and 2(b) before the hydrodynamic field was connected $(\delta_x=0, \delta_z=0)$. This was done following the Levenberg-Marquardt method [21]. Finally, V_x and V_z were fitted to the time series shown in Figs. 2(c) and 2(d), that is, to the functions $V_x=a_0+2\Sigma_{n=1}^{n=2}(a_n^c\cos n\nu_0 t+a_n^s\sin n\nu_0 t)$ and $V_z=b_0+2\Sigma_{n=1}^{n=2}(b_n^c\cos n\nu_0 t+b_n^s\sin n\nu_0 t)$. Note that, although the z coordinate and V_z velocity component show good agreement with the kinematical model; both the x coordinate and V_x velocity component show some imperfections due to the disturbances observed after switching on the gravity field in Figs. 2(b) and 2(d) that were not taken into account in the analysis above.

Figure 3 shows the velocity of the core of the spiral wave as a function of the partial molal volume σ. Note that the two components of the fluid velocity at the core are negative, although the z component is bigger. For small σ, the com-

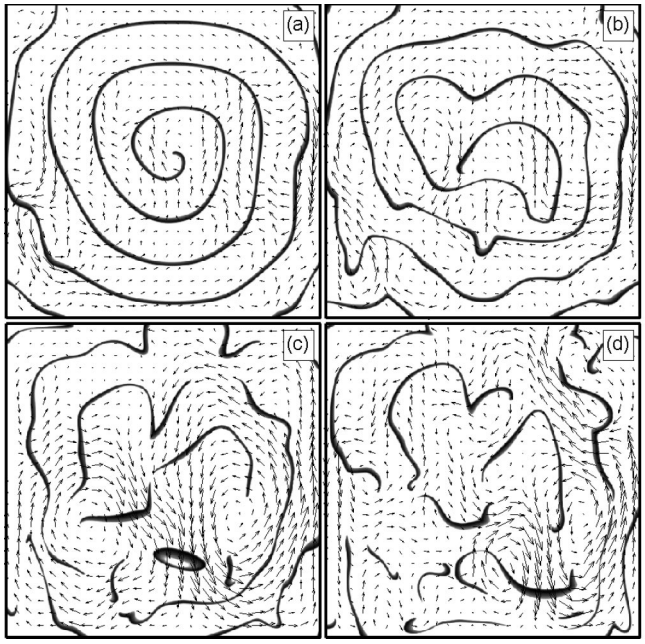

FIG. 4. Time evolution of the spiral breakup induced by the hydrodynamic field, for $\sigma=0.02$. Note the multiple spiral tip formation as a consequence of the wave front breaking. Vortex structures also follow an erratic behavior. Periods of time: (a) 2 t.u., (b) 5 t.u., (c) 7 t.u., and (d) 8 t.u.

ponent of the x direction of the core velocity, within experimental error, is nearly zero. The gradients of density produce some convective flow in the same direction as the gravitational field. Moreover, as $\sigma\rightarrow 0$, the convective flow does not perturb the normal (circular) motion of the spiral tip as both components of the core velocity tend to zero.

When the value of σ is increased above some critical value ($\sigma>0.01$), the spiral is not able to follow the stream as a whole and breaks into pieces. This mechanism of induced spiral breakup is exemplified in the sequence of pictures in Fig. 4. Note that, once the hydrodynamic effects are considered, the spiral becomes loose and arms collide with each other, breaking into pieces and resulting in a very disordered configuration with many free ends. At the same time, fluid vortices also appear randomly, modifying the existing structures.

IV. DISCUSSION

The spiral waves considered in this paper, while propagating through the medium, produced chemical concentration gradients that induced convective currents in the fluid due to gravity, locally resembling Bénard-type cells. In this way, the whole structure was distorted and moved from its original position.

The lack of measured values of the variation of the densities with the concentration of the different species motivated us to perform a detailed analysis of the values of σ. For all values of $\sigma(\rho<\rho_0)$, the spiral drifts follow gravity with a component of the motion in the perpendicular direction that depends on spiral chirality. The reason for this is that, although the tip tends to move upward, there is a stream of fluid going downward that forces the spiral to move downward as observed in Fig. 1. This is clearly seen when the perpendicular component of the motion is analyzed. When a spiral drifts under the effect of an external forcing [24] a counterclockwise spiral (like the one in Fig. 1) has a component of the motion perpendicular to the forcing field direction to the right. In our case, the spiral, due to gravity, tends to move upward with a perpendicular component to the left and, superimposed on all this, the streams in the fluid impose an additional motion to the tip but downward this time. Thus, the global dynamics result in a displacement downward plus a perpendicular component of the motion to the left.

When σ reaches a critical value, the convective streams are so strong that spiral breakup is observed. The rotation frequency of the spiral wave does not change for the values of σ studied; thus the value of the frequency is always supported by the medium and the spiral breakup can be attributed to the coupling of the spiral tip motion with the convective streams. For small values of σ the convective streams are so weak that no effect can be observed. But for large values of σ the streams are so strong that they may destroy the arms of the spiral, inducing a turbulent structure in the medium.

The dispersion of the chemical components within the system is so strong that they induce values for the local curvature in the wave front larger that the critical one, thus breaking up the wave front. These results explain the experiment described in [25] on the appearance of chaotic regimes in a tilted Petri dish only in the deep part of the reagent, where Bénard cells appear. The appearance of the turbulence as described in this paper is different from that described by other authors [26]; here the global variation of the excitability of the medium was the origin for turbulence.

As shown in Eq. (13), the effect of gravity is introduced through the product $g\sigma$. Although we have considered the case where g is constant and σ varies, similar results would be obtained if σ were held constant and g allowed to change in order to obtain the same values of $g\sigma$. This could be useful in understanding cardiac dysrhythmias, in particular those giving rise to multiple reentry formation, when the subject is under extreme acceleration forces ($+Gz$) for significant periods of time [27]. This paper also opens the possibility of further experimental research as experiments can be performed using the Belousov-Zhabotinsky reaction.

ACKNOWLEDGMENTS

We acknowledge Professor J. L. F. Porteiro for helpful comments. This work was supported by MCyT under Research Grant No. BFM2000-0348.

[1] A.M. Turing, Philos. Trans. R. Soc. London, Ser. B **237**, 37 (1952); J.D. Murray, *Mathematical Biology* (Springer-Verlag, Berlin, 1989); M.H. Cohen and A. Robertson, J. Theor. Biol. **31**, 119 (1971); P.N. Devreotes, M.J. Potel, and S.A. MacKay, Dev. Biol. **96**, 405 (1983).

[2] A.N. Zaikin and A.M. Zhabotinsky, Nature (London) **255**, 535 (1970); A.T. Winfree, Science **175**, 634 (1972); *Chemical Waves and Patterns*, edited by R. Kapral and K. Showalter (Kluwer, Dordrecht, 1995); S.K. Scott, *Chemical Chaos* (Oxford University Press, New York, 1991).

[3] M.A. Allesie, F.I.M. Bonke, and F.G.J. Schopman, Circ. Res. **33**, 54 (1973); R.A. Gray and J. Jalife, Int. J. Bifurcation Chaos Appl. Sci. Eng. **6**, 415 (1996).

[4] V. Pérez-Muñuzuri, R. Aliev, B. Vasiev, V. Pérez-Villar, and V.I. Krinsky, Nature (London) **353**, 740 (1991); V. Pérez-Muñuzuri, R. Aliev, B. Vasiev, and V.I. Krinsky, Physica D **56**, 229 (1992); O. Steinbock, V.S. Zykov, and S.C. Müller, Nature (London) **366**, 322 (1993); A.P. Muñuzuri, M. Gómez-Gesteira, V. Pérez-Muñuzuri, V.I. Krinsky, and V. Pérez-Villar, Phys. Rev. E **50**, 4258 (1994).

[5] I. Sendiña-Nadal, S. Alonso, V. Pérez-Muñuzuri, M. Gómez-Gesteira, V. Pérez-Villar, L. Ramírez-Piscina, J. Casademunt, J.M. Sancho, and F. Sagués, Phys. Rev. Lett. **84**, 2734 (2000); V. Pérez-Muñuzuri, F. Sagués, and J.M. Sancho, Phys. Rev. E **62**, 94 (2000).

[6] D.A. Vázquez, J.W. Wilder, and B.F. Edwards, Phys. Fluids A **4**, 2410 (1992); J. Chem. Phys. **98**, 2138 (1993); J.W. Wilder, D.A. Vásquez, and B.F. Edwards, Phys. Rev. E **47**, 3761 (1993); D.A. Vásquez, J.M. Littley, J.W. Wilder, and B.F. Edwards, *ibid.* **50**, 280 (1994); Y. Wu, D.A. Vásquez, B.F. Edwards, and J.W. Wilder, *ibid.* **51**, 1119 (1995); D.A. Vásquez and C. Lengacher, *ibid.* **58**, 6865 (1998).

[7] J.A. Pojman and I.R. Epstein, J. Phys. Chem. **94**, 4966 (1990); J.A. Pojman, I.R. Epstein, and T. McManus, *ibid.* **95**, 1299 (1991); J.A. Pojman, I.R. Epstein, and I. Nagy, *ibid.* **95**, 1306 (1991); J.A. Pojman, R. Craven, A. Jhan, and W. West, *ibid.* **96**, 7476 (1992); I.P. Nagy and J.A. Pojman, *ibid.* **97**, 3443 (1993).

[8] J.I. Ramos, Chaos Solitons Fractals **12**, 1897 (2001); **12**, 2267 (2001).

[9] V.N. Biktashev *et al.*, Phys. Rev. Lett. **81**, 2815 (1998); Phys. Rev. E **60**, 1897 (1999).

[10] T. Sakurai, H. Miike, and E. Yokoyama, in *Proceedings of the 4th Experimental Chaos Conference*, edited by M. Ding, W. Ditto, L. Pecora, M. Spano, and S. Vohra (World Scientific, Singapore, 1997), p. 25.

[11] V. Pérez-Villar, A.P. Muñuzuri, and V. Pérez-Muñuzuri, Phys. Rev. E **61**, 3771 (2000).

[12] S. Chandrasekhar, *Hydrodynamic and Hydromagnetic Stability* (Dover, New York, 1961).

[13] R.J. Field, E. Körös, and R.M. Noyes, J. Am. Chem. Soc. **94**, 8649 (1972).

[14] K. Showalter, J. Phys. Chem. **85**, 440 (1981).

[15] J. Tyson and P.C. Fife, J. Chem. Phys. **73**, 2224 (1980).

[16] J.J. Tyson, in *Oscillations and Traveling Waves in Chemical Systems*, edited by R.J. Field and M. Burger (Wiley-Interscience, New York, 1985).

[17] J.J. Taboada, A.P. Muñuzuri, V. Pérez-Muñuzuri, M. Gómez-Gesteira, and V. Pérez-Villar, Chaos **4**, 519 (1994).

[18] Z. Nagy-Ungvarai, S.C. Müller, T. Plesser, and B. Hess, Naturwissenschaften **75**, 87 (1988).

[19] J.D. Dockery, J.P. Keener, and J.J. Tyson, Physica D **30**, 177 (1988).

[20] W. Jahnke and A.T. Winfree, Int. J. Bifurcation Chaos Appl. Sci. Eng. **1**, 445 (1991); A.T. Winfree, Chaos **1**, 303 (1991).

[21] W.H. Press, S.A. Teukolsky, W. T. Vetterling, and B. P. Flannery, *Numerical Recipes in C*, 2nd ed. (Cambridge University Press, Cambridge, England, 1992).

[22] W. Jahnke, W.E. Skaggs, and A.T. Winfree, J. Phys. Chem. **93**, 740 (1989).

[23] A.S. Mikhailov, *Foundations of Synergetics I* (Springer-Verlag, Berlin, 1994).

[24] A.P. Muñuzuri, M. Gómez-Gesteira, V. Pérez-Muñuzuri, V.I. Krinsky, and V. Pérez-Villar, Phys. Rev. E **48**, 3232 (1993).

[25] K.I. Agladze, V.I. Krinsky, and A.M. Pertsov, Nature (London) **308**, 835 (1984).

[26] M. Bär and M. Eiswirth, Phys. Rev. E **48**, 1635 (1993).

[27] J.E. Whinnery, Aviat., Space Environ. Med. **61**, 716 (1990); I. McKenzie and K.K. Gillingham, *ibid.* **64**, 687 (1993).